

Symmetry breaking in the linear configurations of SX₂ (X=F, Cl, Br, I): Pseudo-Jahn-Teller effect parameters, hardness and electronegativity

Ali Esmaili^a, Reza Fazaeli*^b and Esmat Mohammadi Nasab^a

^aDepartment of Chemistry, Arak Branch, Islamic Azad University, Arak, Iran

^bDepartment of Chemistry, South Tehran Branch, Islamic Azad University, Tehran, Iran

Received: November 2019; Revised: December 2019; Accepted: January 2020

Abstract: The instability of the curved structure in SX₂(X=F,Cl,Br,I) molecules due to the pseudo Jahn-Teller effect(PJTE) was investigated as an original PJTE study, which were bent in the ground state and linear in their first excited state. The effective parameters in vibronic coupling between reference states [HOMO(Π_u) \rightarrow LUMO(Σ_g)] have been investigated in linear structures(D ∞ h). Calculations at the B3LYP/Def2-TZVPP level of theory produced the structural parameters, corrected electronic energies, electronegativity and hardness. The natural bond orbital (NBO) interpretation is associated with [Lp(3)X \rightarrow $\sigma^*(1)S-X$] to obtain stabilization energy (E(2)), vibronic coupling constant(F_{ij}) and energy gaps between reference states(Δ). The interactions and effectiveness of these parameters with the structural parameters of the desired compounds were the focus of the study. In all above mentioned molecules stability were increased with the reduction in the symmetry level. The hardness difference parameter $\Delta[\eta(C2V) - \eta(D\infty h)]$ decreases from F to I (44.05, 37.13, 30.19, 25.14 Kcal/mol). These changes could explain the trend, which were observed for the D ∞ h \rightarrow C2V conversion process.

Keywords: Pseudo-Jahn-Teller effect, vibronic coupling constant, The natural bond orbital, Stabilization energy.

Introduction

These investigations indicate that the cause of the deviation from the linear structure in these combinations is the PJT-effect (PJTE). This effect converts high symmetry configurations in to low symmetry ones. In such system, electron transfer from the highest occupied molecular orbitals (HOMO) to the lowest unoccupied molecular orbitals (LUMO) changes the entire electron configuration. PJTE is a vibronic effect in which electronic transfer will be permitted by the presence of vibrational functions in the torque of the mutation associated with the electron transfer [1-4].

The Jahn-Teller (JT) effect is one of the most fascinating researches of structure distortions that has been widely considered in experimental and theoretical studies for several years [5]. Three types of JT distortions are the JT distortions of molecules in a degenerate electronic ground state, Pseudo JT (PJT) distortions in nondegenerate electronic states, and Renner-Teller (RT) distortions in a linear system [6]. Any structural distortion of a polyatomic system is a consequence of the JT, PJT, or RT effects. Several theoretical investigations have been published about pseudo JT (PJT) distortions in organic and inorganic compounds [7-22]. Such electron delocalizations are investigated for the compounds of interest in this research using the TD-DFT method [23-28].

PJTE theory and formulas are well established. In a two-level problem, the specified ground and excited

*Corresponding author: Tel: +982177248534; Tel.: +989128595684, Email: r_fazaeli@azad.ac.ir

electronic states are mixed in the direction of normal displacement (Q). The symmetry of the electronic wave functions and nuclear displacements are two factors affecting this mixing. The instability of any molecular system is determined by estimating the curvature of the adiabatic potential energy surface (APES). For a high symmetry configuration, the minimum APES is positive, meaning that the value of $K > 0$. If $K < 0$, the molecular system with high symmetry become unstable. According to second-order perturbation theory, the value of K for each molecular system in the electronic nondegenerate states due to small nuclear displacements can be obtained from the following equation:

Equation (1):

$$K = \left\langle \Psi_i \left| \left(\frac{\partial^2 H}{\partial Q^2} \right)_0 \right| \Psi_j \right\rangle - 2 \sum_n \frac{|\langle \Psi_i | \left(\frac{\partial H}{\partial Q} \right)_0 | \Psi_j \rangle|^2}{(E_j - E_i)} \quad (1)$$

The first term in equation (1) is the primary force constant (K_0) and the second term is the vibronic interaction of the ground Ψ_i and excited Ψ_j state wave functions under nuclear displacement (K_v).

$$K_v = -2 \sum_i \frac{F_{ij}^2}{E_j - E_i} \quad (2)$$

The value of the vibronic coupling constant (F_{ij}) as an off-diagonal element can be calculated from Equation (3).

$$F_{ij} = \left\langle \Psi_i \left| \left(\frac{\partial H}{\partial Q} \right)_0 \right| \Psi_j \right\rangle \quad (3)$$

E_i and E_j in Equation (2) are the energies of the ground and excited states.

Results and discussion

Energetic aspects

For any polyatomic systems with high symmetry configuration, two or more electronic states interact under nuclear displacement and these interactions lead to instability. In the case of the above mentioned molecules inappropriate displacement of donor and acceptor orbitals in the linear structures create a radial knot and therefore an electron delocalization which will not be allowed. So the system has been distorted to remove this radial knot so electron delocalization would be allowed (Figure 1). At the linear structure $Q=0$, given that distortion does not occur under nuclear displacement. During the curvature, the system gains energy and undergoes a deformation which can be seen by the change in bond length, bond angle.

The structures of molecules sulfur difluoride (1), sulfur chloride (2), sulfur bromide (3) and sulfur iodide (4) were optimized at the B₃LYP/Def2-TZVPP level of theory in the linear ($D_{\infty h}$) and the curved (C_{2v}). Table (1) represents the absolute energy of these molecules. The vibrational analysis of the symmetry ($D_{\infty h}$) shows four imaginary frequencies. Table (2) provides the values of these frequencies and their force constant. It can be indicated by the symmetry of the vibrational modes of these imaginary frequencies, which are (Π_u). Figure 1 shows these vibrational modes. It can be observed that these vibrational modes change the symmetry of the linear molecule ($D_{\infty h}$) to the curved (C_{2v}). The distortions of high symmetry ($D_{\infty h}$) configurations of compounds are caused by the PJTE.

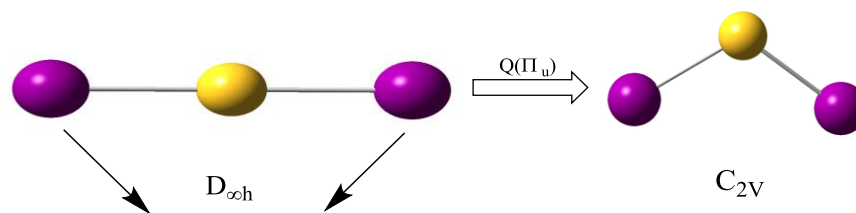
Table 1: Absolute energy (a.u), relative energy (kcal mol⁻¹), Structural parameters of linear ($D_{\infty h}$) and distorted (C_{2v}) configurations at B₃LYP/Def2-TZVPP level of theory for 1 to 4.

Compound	E_0	ΔE	r_{S-X}	$\Delta[r_{S-X}(D_{\infty h}) - r_{S-X}(C_{2v})]$	θ_{S-X-S}	$\Delta[\theta_{S-X-S}(D_{\infty h}) - \theta_{S-X-S}(C_{2v})]$
SF ₂						
C_{2v}	-597.942923	0.0	1.6051	0.077	98.728	81.27
$D_{\infty h}$	-597.856811	54.036	1.6824		180.0	
SCL ₂						
C_{2v}	-1318.662194	0.0	2.0390	0.130	104.130	75.87
$D_{\infty h}$	-1318.579631	51.244	2.1696		180.0	
SBr ₂						
C_{2v}	-5546.584767	0.0	2.2067	0.132	105.359	74.64
$D_{\infty h}$	-5546.510188	46.80	2.3386		180.0	
SI ₂						
C_{2v}	-993.838783	0.0	2.4088	0.137	106.870	73.13
$D_{\infty h}$	-993.769122	43.713	2.5463		180.0	

Table 2: Calculating vibrational frequencies(cm^{-1}) of compounds 1-4.

Compound	SF ₂	SCl ₂	SBr ₂	SI ₂
ν_1	-386.6320	-323.6811	-282.2956	-289.3103
Force constant	2.1462	2.0281	1.6683	1.7207
Δ	2.84	0.93	0.57	0.08

Figure 1: Schematic representation of SX₂(D_{∞h}) along nuclear displacement Q_(Π_u) and the curved(C_{2v}) configuration of compounds 1 to 4.



The term symbol of the ground state of the (D_{∞h}) symmetry for the studied molecules is (Σ_g). The main influences of the distortions of high symmetry (D_{∞h}) configurations to their corresponding (C_{2v}) form of compounds are mainly due to the PJTE by mixing the ground (Σ_g) and excited (Π_u) states associated with the mixing of $\Psi_{\text{HOMO}}(\Sigma_g)$ and $\Psi_{\text{LUMO}}(\Pi_u)$ orbitals in studied compounds resulting in a PJT($\Sigma_g + \Pi_u$) $\times \Pi_u$ problem.

The results of the calculations show that the main contributions to these excited states are attributed to HOMO (Π_u) \rightarrow LUMO(Σ_g) transitions.

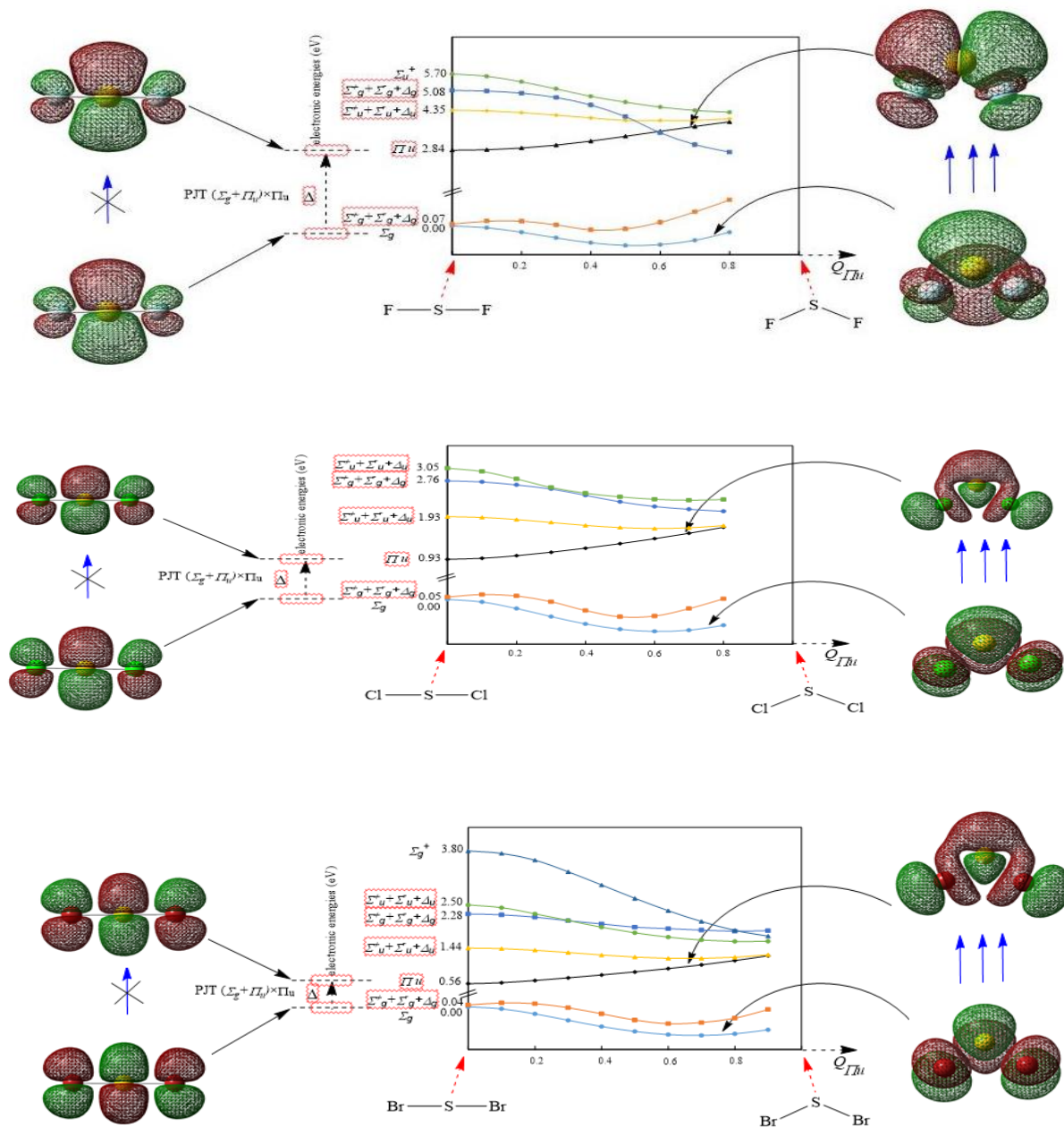
The energies of the ground and excited states and their change along the distortion coordinate [Q_(Π_u)] are shown in Fig.2. As shown in Fig.2, the curvatures of the lower curves (corresponding to the ground state electronic configurations) of the adiabatic potential energy surface (APES) become negative, but in the upper curve (corresponding to the excited electronic

configurations which interact with the lower curve with respect to Q_(Π_u) displacements) the curvatures become positive. These calculations show that the minimum energy values along the distortion coordinate are observed as 0.5(X=F), 0.6(X=Cl), 0.7(X=Br) and 0.8(X=I). The difference between these minimum energy values and the (D_{∞h}) symmetry energy values are the JT effect energy (E_{JT}). These values are listed in Table 3. They decrease with decreasing electronegativity of the substituent. A good linear association between E_{JT} and Pauling electronegativity (χ_p) of halogens can be found:

$$E_{\text{JT}} = 3.98 \text{ (F)} - 3.16 \text{ (Cl)} - 2.96 \text{ (Br)} - 2.66 \text{ (I)} - \chi_p$$

$$E_{\text{JT}} = 7.5961\chi_p + 25.131 \quad R^2 = 0.875$$

Therefore, there is a stronger Jahn-Teller effect in the increase of electronegative halogens and OF₂ is more stable due to the Jahn-Teller effect.



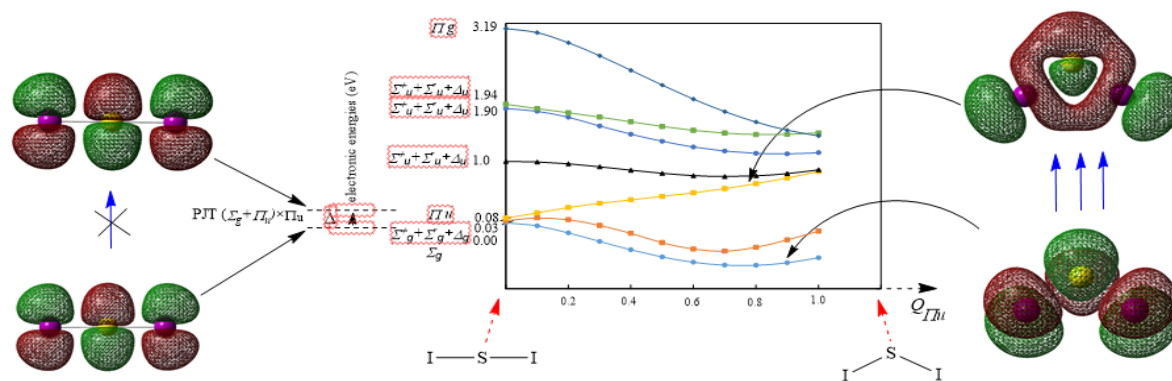


Figure 2: Energies of the ground and excited states and their change along the distortion coordinate $Q(\Pi_u)$ of SX_2 molecules in the $(D_{\infty h})$.

Table 3: Minimum Absolute Energy Along the coordinate of the (Π_u) Vibration, Minimum Energy Point(\AA) and JT Stabilization Energy(E_{JT} ,Kcal/mol)of SX_2 molecules($X=F, Cl, Br, I$) at the B3LYP/Def2-TZVPP level of theory.

Compound	r_{\min}	E(min)	E_{JT}
SF ₂	0.5	-597.9474138	54.48
SCl ₂	0.6	-1318.6640357	51.71
SBr ₂	0.7	-5546.5868663	47.21
SI ₂	0.8	-993.8405051	44.05

Structural Parameters

S-X bond distances, and X-S-X bond angles in the studied molecules are listed in Table (1). It can be found that the most change in bond distances and bond angles occur during a decrease in the symmetry from $(D_{\infty h})$ to (C_{2v}) in the presence of halogens ($X=F, Cl, Br, I$). Table (1) shows that X-S-X bond angle increase with decreasing electronegativity of halogen.

It can be found that bond distances are shorter in (C_{2v}) symmetry compared to $(D_{\infty h})$ symmetry. Table (1) shows that X-S-X bond angles are decreased with the decreased of symmetry.

As shown in Table (1), $\Delta[r_{S-X}(D_{\infty h}) - r_{S-X}(C_{2v})]$ increases with decrease electronegativity of halogen. The variation of the θ_{X-S-X} bond angle in the effect of distortion of $(D_{\infty h})$ structures to (C_{2v}) structures decreases with the decrease of the electronegativity of halogens. A good linear correlation between E_{JT} and $\Delta[\theta_{X-S-X}(D_{\infty h}) - \theta_{X-S-X}(C_{2v})]$ can be observed:

$$\Delta[\theta_{X-S-X}(D_{\infty h}) - \theta_{X-S-X}(C_{2v})] = 0.6946 E_{JT} + 41.942; R^2 = 0.8268$$

Molecular orbital analysis

According to Koopmans' theorem, the frontier orbital energies are:

$$\chi = -(\epsilon_{LUMO} + \epsilon_{HOMO})/2 \quad (4)$$

$$\eta = (\epsilon_{LUMO} - \epsilon_{HOMO})/2 \quad (5)$$

Table (4) provides the energies of the frontier orbitals (HOMO, LUMO), the corresponding HOMO-LUMO energy gaps and the global hardness values and the global electronegativity values of the investigated molecules.

As shown in Table (4), HOMO energy values increase with the decrease of the electronegativity of halogen in the molecules. In contrast, LUMO energy values decrease with decreasing of electronegativity of halogens in the molecules.

Moreover, HOMO-LUMO gap and the global hardness of (C_{2v}) symmetry are higher than those of $(D_{\infty h})$ symmetry. As estimated from the minimum energy principles (MEP), and maximum hardness (MHP), while a conformer changes from the most steady to other less stable species in most cases, the energy increases and the hardness reduces [31-35]. Also, HOMO-LUMO gap values are dependent on the character of the substituent. With the decrease of electronegativity of the halogen, these values are decreasing. A good linear relation between the HOMO-LUMO gap and Pauling electronegativity (χ_p) of halogens can be indicated:

$$\text{Gap} = 1.4599\chi_p - 0.7272; R^2 = 0.9346$$

Table 4: B3LYP/Def2-TZVPP calculated energy (in au) of HOMO, LUMO, LUMO-HOMO (in au), global hardness (η , in au), global electronegativity (χ , in au), $\Delta\eta$ (in kcal mol⁻¹) and $\Delta\chi$ ((in kcal mol⁻¹) parameters for the curved (C_{2v}) ground state and linear (D_{∞h}) structures of compounds 1-4.

Geometry	ϵ_{HOMO}	ϵ_{LUMO}	$\epsilon_{\text{LUMO}}-\epsilon_{\text{HOMO}}$	η	χ	$\Delta\eta$	$\Delta\chi$
SF ₂ , C _{2v}	-0.25904	-0.07630	4.97	2.48	0.16767	1.91(44.05) ^a	-0.0868(-54.49) ^a
SF ₂ , D _{∞h}	-0.27565	-0.23338	1.15	0.57	0.254515	0.00000	0.00000
SCl ₂ , C _{2v}	-0.25568	-0.10131	4.20	2.10	0.178495	1.61(37.13) ^a	-0.07507(-47.11) ^a
SCl ₂ , D _{∞h}	-0.27154	-0.23560	0.98	0.49	0.25357	0.00000	0.00000
SBr ₂ , C _{2v}	-0.25193	-0.12076	3.57	1.78	0.186345	1.34(30.90) ^a	-0.06087(-38.19) ^a
SBr ₂ , D _{∞h}	-0.26372	-0.23072	0.89	0.44	0.24722	0.00000	0.00000
SI ₂ , C _{2v}	-0.24081	-0.13137	2.98	1.49	0.18609	1.09(25.14) ^a	-0.04709(-29.55) ^a
SI ₂ , D _{∞h}	-0.24792	-0.21845	0.80	0.40	0.233185	0.0000	0.00000

Moreover, the variations of hardness in the effect of the symmetry descending show a good correlation with E_{JT}:

$$[\eta(\text{C}_{2\text{V}})-\eta(\text{D}_{\infty\text{h}})]=0.5667 E_{\text{JT}}+29.92; R^2=0.9878$$

It has to be noted that the global electronegativity, χ , determines the Lewis acid or Lewis base character of a molecule. Molecules with large χ values are characterized as strong Lewis acids and small χ values are found for strong Lewis bases. Table (4) shows that, compound **1**(SF₂) is considered as a stronger Lewis acid, and compound **4** (SI₂) as a stronger Lewis base amongst the compounds **1** to **4**. The calculation the parameter $\Delta[\chi(\text{C}_{2\text{V}})-\chi(\text{D}_{\infty\text{h}})]$ it is observed that this parameter increase the compounds **1** to **4**, and showed a good linear correlation with E_{JT}. $\Delta[\chi(\text{C}_{2\text{V}})\chi(\text{D}_{\infty\text{h}})]=0.4279E_{\text{JT}}+31.249$; $R^2=0.9958$

Natural bond orbital (NBO) analysis

In this section we discuss the illustrated distortion of the studied molecules based on the calculated parameters from the NBO analysis.

Table (5) reports the largest second-order interaction energies E⁽²⁾ between the donor and acceptor orbitals in the studied molecules. The second-order Fock matrix was utilised to estimate the interactions of the donor-acceptor in the NBO analysis. For each donor (i) and acceptor (j), the stabilisation energy E⁽²⁾ related to the delocalisation i→j is evaluated as:

$$E^{(2)} = -q_i \frac{F^2(i,j)}{\epsilon_j - \epsilon_i} \quad (6)$$

Where q_i is the donor occupied orbital, ϵ_i and ϵ_j correspond to the donor and acceptor orbitals, respectively. $\epsilon_j - \epsilon_i$ is the energy difference between the donor and acceptor orbitals. F_{ij} is the nondiagonal element. The larger the E⁽²⁾ value denotes the significant interaction between electron donors and electron acceptors. The results obtained from the calculations show that the stabilization energies associated with electron delocalization [Lp(3)_x→σ*(1)_{s-x}] in the curved structures decrease from **1** to **4**.

The differences between the E⁽²⁾ values for these structures decrease with the decrease of the electronegativity of halogens. A good linear correlation between E_{JT} and $[E^{(2)}(\text{C}_{2\text{V}}) - E^{(2)}(\text{D}_{\infty\text{h}})]$ values can be observed: $[E^{(2)}(\text{C}_{2\text{V}}) - E^{(2)}(\text{D}_{\infty\text{h}})] = 0.6538E_{\text{JT}} + 62.974$; $R^2=0.9532$

The second parameter that effected the stabilization energies E⁽²⁾ is the diagonal Fock matrix elements (vibronic coupling constant; F_{ij}). The calculated values (F_{ij}) for electron delocalization [Lp(3)_x→σ*(1)_{s-x}] for compounds **1** to **4** were 0.071, 0.052, 0.044 and 0.036 a.u., respectively (Table 5). As expected, it shows a decreasing trend from **1** to **4**. The second parameter that effected the stabilization energies is the diagonal matrix elements (energies of bonding and anti-bonding orbitals). Unlike F_{ij}, they have reverse relevance E⁽²⁾. As seen shown in Table 5, the energy of the strong anti-bonding acceptor orbitals and energy of the strong bonding donor orbitals increasing for compounds **1** to **4**.

Table 5: Calculated stabilization energies ($E^{(2)}$ in Kcal mol⁻¹), orbital occupancy (q_i), off-diagonal elements (F_{ij} , in a.u.), orbital energies (ϵ , in a.u.) using the NBO- B3LYP/Def2-TZVPP method for the curved (C_{2v}) configurations 1 to 4.

Compound	SF ₂	SCl ₂	SBr ₂	SI ₂
$E^{(2)}$				
Lp(3) _X → $\sigma^*(1)_{S-X}$	15.42	14.38	12.65	10.16
Orbital occupancy				
Lp(3) _X	1.90031	1.87963	1.87970	1.88508
$\sigma^*(1)_{S-X}$	0.08151	0.10958	0.11219	0.10945
F_{ij}				
Lp(3) _X → $\sigma^*(1)_{S-X}$	0.071	0.052	0.044	0.036
ϵ				
Lp(3) _X	-0.48839	-0.37989	-0.35063	-0.31290
$\sigma^*(1)_{S-X}$	-0.08503	-0.14644	-0.15832	-0.15446
$\Delta(E \text{ Lp}(3)_X \rightarrow E\sigma^*(1)_{S-X})$	0.40336	0.23345	0.19231	0.15844

Conclusions

In this investigation, we studied the instability of linear structure in SX_2 (X=F, Cl, Br, I) molecules at the B3LYP/Def2-TZVPP level of theory and observed the following: 1-In the studied molecules, descending of symmetry increased the stability of the molecule. This increase of stability is associated with the PJTE. 2-The vibronic coupling interaction between the (Σ_g) ground and the first (Π_u) excited states through the PJT ($\Sigma_g + \Pi_u$) × Π_u PJTE problem was the causes of the symmetry breaking phenomenon and the curved in the studied molecules.

3-The increased stability of C_{2v} structures in compared to $D_{\infty h}$ structures were compatible with the principles of minimum energy (MEP), and maximum hardness (MHP). 4-The differences between the $E^{(2)}$ values of strongest interaction for these structures decrease with decreasing of electronegativity of halogen and showed a good linear correlation with E_{JT} .

Computational Methods

All calculations were performed with the Gaussian09 program suite [29]. The standard Def2-TZVPP basis set was used in the calculations [30]. Using the hybrid functional of the B3LYP method, geometry optimization was conducted at each stationary point found, confirming its identity as an energy minimum. The correlations between structural parameters and PJT parameters were investigated using natural bond orbital (NBO) interpretations [31].

Acknowledgements

We gratefully acknowledge financial support from the Research Council of Islamic Azad University of

Yazd and the Islamic Azad University of Zahedan of Iran.

References

- [1] Bersuker, I. B., *Chem. Rev.* **2001**, *101*, 1067.
- [2] Bersuker, I. B.; *The Jahn-Teller Effect* Cambridge University Press: Cambridge, UK **2006**.
- [3] Bersuker, I. B.; *Chem. Rev.* **2013**, *113*, 1351.
- [4] Bersuker, I. B. *Phys. Rev. Lett.* **2012**, *108*, 137202(1)-137202(2).
- [5] Burke, K, Werschnik, J, Gross, E. U, *J. Chem. Phys.* **2005**, *123*, 062206.
- [6] Bauernschmitt, R.; Ahlrichs, R. *Chem. Phys. Lett.* **1996**, *256*, 454.
- [7] Mahmouzdadeh, G.; Ghiasi, R.; Pasdar, H. *J. Structural Chemistry*, **2019**, *60*, 736.
- [8] Hajhoseinzadeh, K.; Ghiasi, R.; Marjani, A. *Eurasian Chem. Commun.* **2020**, *2*, 78.
- [9] Faramarzi, E.; Ghiasi, R.; Abdoli-Senejani, M.; *Eurasian Chem. Commun.* **2020**, *2*, 187.
- [10] Vafaei-Nezhad, M.; Ghiasi, R.; Shafiei, F. *Chem. Methodol.* **2020**, *4*, 161.
- [11] Ghorbaninezhad, S.; Ghiasi, R. *Chem. Methodol.* **2020**, *4*, 80.
- [12] Shalmani, G. G.; Ghiasi, R.; Marjani, A. *Chem. Methodol.* **2019**, *3*, 752.
- [13] Ghiasi, R.; Hakimioun, A. H. *Iran. Chem. Commun.* **2017**, *5*, 67.
- [14] Ghiasi, R.; Monajjemi, M.; Mokarram, E. E.; Makkipour, P. *J. Struct. Chem.* **2008**, *49*, 600.
- [15] Ghiasi, R.; Pasdar, H. *Russ. J. Phys. Chem. A*, **2013**, *87*, 973.
- [16] Ghiasi, R.; Pasdar, H.; Irajzadeh, F. *J. Chilean Chem. Soc.* **2015**, *60*, 2740.
- [17] Ghiasi, R.; Zafarniya, F.; Ketabi, S. *Russ. J. Inorg. Chem.* **2017**, *62*, 1371.
- [18] Ghiasi, R.; Heidarbeigi, A. *Russ. J. Inorg. Chem.* **2016**, *61*, 985.

- [19] Rezazadeh, M.; Ghiasi, R.; Jamehbozorgi, S. *J. Struct. Chem.* **2018**, *59*, 245.
- [20] Mahmoudzadeh, G.; Ghiasi, R.; Pasdar, H. *Russ. J. Phys. Chem. A*, **2019**, *93*, 2244.
- [21] NajjariMilani, N.; Ghiasi, R.; Forghaniha, A. *J. Sulfur Chem.* **2018**, *39*, 665.
- [22] Esmaeili, A.; Fazaeli, R.; MohammadiNasab, E. *Eurasian Chem. Commun.*, **2020**, 2, 739.
- [23] Burke, K.; Werschnik, J.; Gross, E. U. *J. Chem. Phys.* **2005**, *123*, 062206.
- [24] Bauernschmitt, R.; Ahlrichs, R.; *Chem. Phys. Lett.*, **1996**, *256*, 454.
- [25] Casida, M. E.; Jamorski, C.; Casida, K. C.; Salahub, D. R. *J. Chem. Phys.*, **1998**, *108*, 4439.
- [26] Marques, M. A. L.; Gross, E. K. U. *Ann. Rev. Phys. Chem.* **2004**, *55*, 427.
- [27] Dufty, J.; Luo, K.; Trickey, S. B.; *Phys. Rev. E*. **2018**, *98*, 033203.
- [28] Ning, Z.; Liang, C. T.; Chang, Y. C. *Phys. Rev. B*. **2017**, *96*, 085202.
- [29] Frisch, M. J.; Trucks, G. W.; Schlegel, H. B.; Scuseria, G. E.; Robb, M. A.; Gaussian 09, Revision A.02; Gaussian, Inc.: Wallingford CT, **2009**.
- [30] Frisch, M. J.; Trucks, G. W.; Schlegel, H. B.; Scuseria, G. E.; Robb, M. A.; Cheeseman, J. R.; Scalman, G.; Barone, V.; Mennucci, B.; Petersson, G. A.; Nakatsuji, H.; Caricato, M.; Li, X.; Hratchian, H. P.; Izmaylov, A.; Bloino, J.; Zheng, G.; Sonnenberg, J. L.; Hada, M.; Ehara, M.; Toyota, K.; Fukuda, R.; Hasegawa, J.; Ishida, M. T.; Nakajima, Honda, Y.; Kitao, O.; Nakai, H.; Vreven, T.; Montgomery, J. A.; Peralta, J. E.; et.al. Gaussian 09, Revision A.02; Gaussian, Inc.: Wallingford CT, **2009**.
- [31] Glendening, E. D.; Badenhoop, J. K.; Reed, A. E.; Carpenter, J. E.; Bohmann, J. A.; Morales, C. M.; Landis, C. R.; Weinhold, F.; NBO6.0: Natural bond orbital analysis program, Theoretical Chemistry Institute, University of Wisconsin, Madison, WI, **2013**.
- [31] Ayers, P. W.; Parr, R. G. *J. Am. Chem. Soc.* **2000**, *122*, 2010.
- [32] Parr, R. G.; Chattaraj, P. K. *J. Am. Chem. Soc.* **1991**, *113*, 1854.
- [33] Pearson, R. G. *J. Chem. Edu.* **1987**, *64*, 561.
- [34] Pearson, R. G. *Acc. Chem. Res.* **1993**, *26*, 250.
- [35] Pearson, R. G. *J. Chem. Edu.* **1999**, *76*, 570.